

Journal of
**Micro/Nanolithography,
MEMS, and MOEMS**

SPIEDigitalLibrary.org/jm3

Design and wafer-level replication of a freeform curvature for polymer- based electrostatic out-of-plane actuators

Nicolas Lange
Sebastian Scheiding
Frank Wippermann
Erik Beckert
Ramona Eberhardt
Andreas Tünnermann

Design and wafer-level replication of a freeform curvature for polymer-based electrostatic out-of-plane actuators

Nicolas Lange

Sebastian Scheiding

Friedrich-Schiller-Universität Jena

Abbe Center of Photonics

Institute of Applied Physics

Max-Wien-Platz 1, D-07743 Jena, Germany

and

Fraunhofer Institute for Applied Optics and

Precision Engineering

Albert-Einstein-Str. 7, D-07745, Jena, Germany

E-mail: Nicolas.Lange@iof.fraunhofer.de

Frank Wippermann

Erik Beckert

Ramona Eberhardt

Fraunhofer Institute for Applied Optics and

Precision Engineering

Albert-Einstein-Str. 7, D-07745, Jena, Germany

Andreas Tünnermann

Friedrich-Schiller-Universität Jena

Abbe Center of Photonics

Institute of Applied Physics

Max-Wien-Platz 1, D-07743 Jena, Germany

and

Fraunhofer Institute for Applied Optics and

Precision Engineering

Albert-Einstein-Str. 7, D-07745, Jena, Germany

Abstract. The purpose of this paper is the fabrication, replication, and wafer-level imprinting of a polynomial curvature to enable the realization of an electrostatic out-of-plane zipper actuator with considerably altered and enhanced voltage versus deflection behavior. This is achievable only by changing silicon as established main material to a UV-curable polymer, while retaining the lithography-based fabrication technology. The basic concept of this actuator is explained, and with derived design rules, a finite element analysis is established to design an actuator with an integrated micro-mirror and 10- μm deflection at 60-V driving voltage. The diamond turning of the master mold and the wafer-level fabrication process of the polynomial curvature are explained in detail and realized by unconventional wafer-level imprinting of a UV-curable, nonconducting polymer. The experimental results of the deflection measurements show a deflection of the intended 10 μm at 200 V. This deviation in necessary driving voltage can be explained by fabrication-induced intrinsic stresses, which bend the actuator beams upward. This increases the gap between the electrodes, making it possible to achieve 26- μm deflection at 300 V. This paper finalizes with an illustration about the now possible designs for polymer-based electrostatic zipper actuators. © The Authors. Published by SPIE under a Creative Commons Attribution 3.0 Unported License. Distribution or reproduction of this work in whole or in part requires full attribution of the original publication, including its DOI. [DOI: [10.1117/1.JMM.12.4.041205](https://doi.org/10.1117/1.JMM.12.4.041205)]

Subject terms: actuators; polymers; lithography; adaptive optics; micro-optics; micro-electromechanical systems.

Paper 13065SS received Apr. 30, 2013; revised manuscript received Oct. 8, 2013; accepted for publication Oct. 23, 2013; published online Nov. 26, 2013.

1 Introduction

Since the electrostatic principle is a surface effect rather than based on the actuator volume, a relatively high energy density can be achieved. Thus, electrostatic actuators are versatile and convenient for miniaturization and integration. They are relatively easy to fabricate and widely utilized in modern microelectromechanical systems (MEMS).¹ Silicon as a base material is still predominant, allowing small, precise, and fast sensors and actuators.² As a stiff material, however, the structures have to be fragile and miniaturized in order to provide a usable deflection for a reasonable actuation voltage and the possibilities of shaping silicon are limited by the according fabrication technology. In addition, the combination with other materials for enhanced functionality (e.g., microlenses) is challenging. It is the intention to maintain wafer-level fabrication, comparable to the wafer-level fabrication of silicon-based MEMS actuators, while scaling up the dimensions of an electrostatic actuator. To fulfill the requirements of mm-scale actuators, thus fitting in the gap between micro- and mm-scale actuators, a different base material than silicon is reasonable for realization. UV-curable polymers exhibit a low elastic modulus, thus allowing less fragile, larger structures and higher deformations for a comparable actuation force. In addition, the fabrication technology of some UV-curable polymers presents the possibility of imprinting complex freeform structures on wafer-level which can be

utilized to create enhanced actuators and functional elements like microlenses or microgrippers. The fabrication technology for such a polymer is still based on classic lithography; therefore, the positioning as well as feature size accuracy and resolution of lithographic photomasks can be achieved. In contrast to silicon, most UV-curable polymers do not possess the properties necessary for actuator functionality themselves. Such can be integrated depending on the chosen principle. As a surface effect, the electrostatic principle is independent of the underlying volume; therefore only two thin metallizations (and an insulation layer eventually) are necessary to integrate electrostatic actuators in polymer-based structures. Therefore, this paper presents the fabrication and actuation results of an imprinted freeform surface for an electrostatic out-of-plane zipper actuator which is completely based on a UV-curable polymer.

1.1 Outline

First, the basic characteristics of a simple zipper actuator are briefly explained. Because of the more complex setup, the whole actuator has to be designed utilizing finite element analysis (FEA). For this, the requirements and the basic idea of the actuator with an integrated micro-mirror, as an example, are described and the design and corresponding FEA results are presented, achieving the intended deflection with no pull-in effect. Consequently,

the previously theoretically designed polynomial curvature has to be fabricated. The whole fabrication and especially the wafer-level imprinting of the polynomial freeform are described in detail. After each process step, the freeform is analyzed and deviations from the design goal are calculated. Subsequently, the deflection of the fabricated actuator was measured and the experimental results are discussed. The conclusion and outlook give a summary of the achieved results and examples describing the potential use of the presented technology for future actuators.

1.2 Principle and Basic Design Rules

The electrostatic principle is widely known and used for actuators and will, therefore, not be explained at this point. The presented actuator is based on the so-called zipper actuator, the fundamentals of a two-dimensional (2-D) zipper actuator are discussed in detail in Refs. 3 and 4. For discussion of the actuator presented in this paper, it is sufficient to point out a few characteristics and basic design rules of an electrostatic actuator, respectively, the zipper actuator. Due to the highly nonlinear force-deflection-correlation, usually only one-third of the whole deflection range of a parallel-plate actuator is usable until the movable electrode is pulled-in.⁵ This also occurs for zipper actuators. The pull-in effect can theoretically be circumvented by specific electrodes resembling a polynomial curvature.³ The degree of that polynomial has great influence on the voltage versus deflection curve. A polynomial with $0 \leq n \leq 2$ leads to a nearly bistable behavior with a distinct pull-in effect. With an increasing degree of the polynomial, the deflection versus voltage behavior becomes more linear at the cost of increased voltage per micrometer deflection.⁴ To obtain an analog deflection behavior with relatively low actuation voltage, the polynomial degree of $n = 3$ will be used for upcoming simulations. Additionally, in Ref. 4, a saturation-like behavior can be observed once the deflection of the cantilever beam gets closer to the maximum deflection. Subsequently, the maximum deflection δ_{\max} should exceed the intended deflection of the actuator for an optimized voltage-deflection ratio. Besides that, the performance (generated force and deflection per volt) of the electrostatic zipper actuator can exceed the more common comb-drive and gap-closing actuators⁶ with a challenging fabrication as downside. Such a polynomial curvature can be created via silicon etching or deposition⁷ and is, due to limitations in fabrication, only suitable for in-plane movement. To ensure electrical insulation, the electrodes defined by the polynomial curvature are often embedded with bumpers for a minimum distance to the flexible cantilever beam,⁸ interrupting the intended curvature, and altering the deflection behavior. Despite those limitations, various design of silicon-based zipper actuators are successfully implemented in several devices such as fluid control⁹ or deformable mirrors.¹⁰ By changing the main material from silicon to a UV-curable polymer it is possible to fabricate three-dimensional (3-D) freeform curvatures with the scope of building out-of-plane zipper actuators with a specific polynomial curvature to alter the voltage versus deflection behavior considerably. For this, the required polynomial freeform has to be precisely replicated. In addition to the heavily changed fabrication possibilities, the elastic modulus of such a polymer [e.g.,Ormocomp® with 1.6 GPa (Ref. 11)] is considerably

lower than the elastic modulus of silicon [160 GPa (Ref. 12)], thus drastically reducing the required voltage.

2 FEA Modeling and Actuator Design

A specific electrode curvature and setup known as the zipper actuator is used for the intended minimization of the pull-in effect and a linearized voltage-deflection behavior of a micro-mirror (1 mm diameter) with an out-of-plane deflection range of 10 μm by equal or <60 V actuation voltage. To be suitable for mobile devices, a maximum diameter of 4 mm for the whole actuator device is set. The zipper actuator presented in this work is similar to a classic design of a zipper actuator.⁴ It is designed as a system of two electrodes, one as a fixed- and curved-bottom electrode, the second as a straight and flexible cantilever beam. The FEA was done with the FEA package CoventorWare from Coventor®. CoventorWare utilizes the boundary element method (BEM). BEM is based on a matrix in which the capacity between all surfaces is stored and consequently, a meshed air volume is not necessary to calculate deformations depending on changes in capacity and force. This allows the simulation of complex contact problems between two (or more) electrodes. To satisfy the specifications of an actuator diameter of equal or <4 mm, three (to assure the stability of the micro-mirror) of the basic 2-D actuators [Fig. 1(a)] were arranged in a circle following the circumference. A flexure hinge between each beam tip and the central micro-mirror area is provided [Fig. 1(b)].

FEA results of the micro-mirror deflection for this design are shown in Fig. 2 with the thickness of the beam as a variable parameter. It is obvious that deflection and required voltage strongly depend on the thickness of the beam.

The intended deflection of 10 μm at 60 V is reached with a beam of 50- μm thickness. With a beam of 30- μm thickness, the required voltage for 10- μm deflection drops even below 27 V.

3 Fabrication Process

For imprinting the beforehand designed freeform curvature, a master mold has to be fabricated and replicated on wafer level. Although this mastering process is time consuming, it is possible to completely imprint an 8 in. wafer with an array of the desired freeform structures (or any other even more complex curvatures). In the process, a stamp is pressed into an initially liquid polymer which hardens under UV-illumination. A master structure of sufficient quality containing the required shape is mandatory for proper replication results. In the case of zipper-type actuator modules, 3-D freeform-like surface shapes are required in order to achieve the intended movement with no pull-in effect and to reduce the driving voltage. The surface profile of a single structure can be manufactured by ultra-precision diamond machining as described below.

As usual in MEMS technology, wafer-based batch techniques are used instead of single devices for better handling and in order to decrease fabrication costs. Consequently, an array-like master structure is required consisting of several identical structures placed on a fixed pitch. As an alternative to the time consuming and, hence expensive fabricating of the whole array by ultra-precision diamond machining, a step and repeat process is used. This process relies on the generation of copies of the stamp containing the single

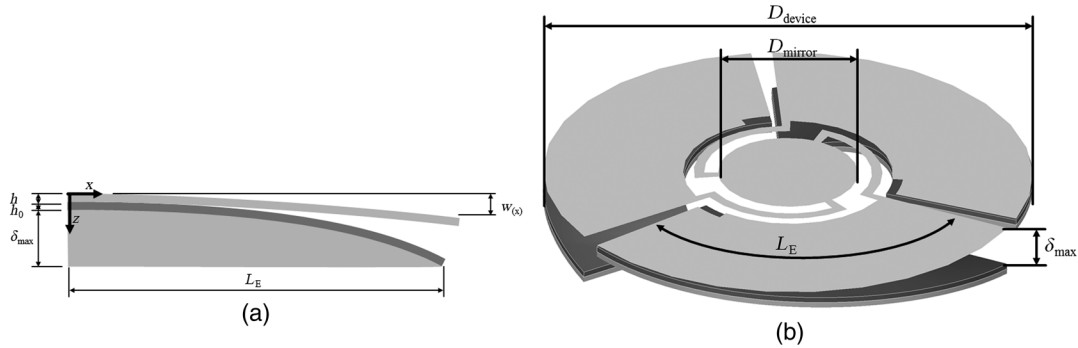


Fig. 1 (a) Illustration of the two-dimensional zipper actuator with assigned symbols. (b) Illustration of the intended zipper actuator design with assigned symbols.

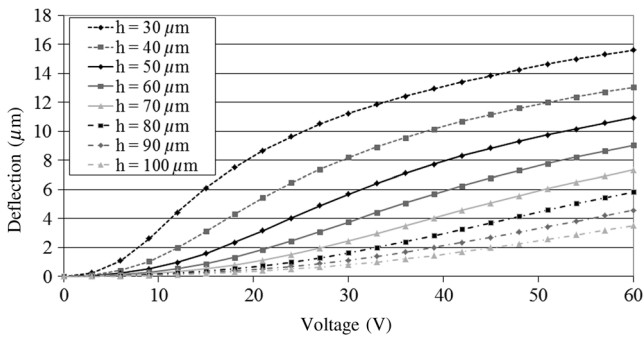


Fig. 2 Simulated deflection at the center of the micro-mirror. At 60 V, the 50- μm thick beam reaches 10.9- μm deflection and fulfills the requirement. With a 30- μm thick beam, the required voltage for 10- μm deflection is below 27 V.

structure by laterally repetitive replication in UV-curing polymers on a common substrate. The whole process for the generation of arrays of almost arbitrary structures depends on a sequence of polymer dispense, single lens tool positioning, imprinting, UV-curing, and mold detaching (Fig. 3).

As depicted in Fig. 3, a transparent stamp (2) is made from a diamond machined brass master (1). Liquid silicone elastomer (Sylgard 184) is cast into the master mold for the fabrication of the transparent stamp. Advantageously, the material vulcanizes at room temperature and possesses very little shrinkage. The drop of liquid silicone is placed on a template glass substrate, which can be loaded into the machine. In the subsequent step and repeat process (3),

the array-like master is produced. Finally, the entire wafer is coated by UV-curing polymer, but illuminated only in the gaps between the micro-structures for planarization (4). Uncured polymer is washed-out after the exposure. From the array master, a replication tool is generated by overcasting with a liquid silicone elastomer (5). Subsequently, the replication tool is used for the UV-replication of the micro-structures on wafer level.

The fabrication of the initial master mold is based on an ultra-precision diamond turning process of a brass tool insert. The diamond turning of the structure takes benefit from the unique properties such as the outstanding hardness, the chemical resistance, the low friction, and the high thermal conductivity of the cutting tool material.¹³

Ultra-precision diamond turning machines are routinely used to fabricate optics with a center of symmetry. Since the 3-D geometry shows no rotational symmetry but high-frequency asymmetric features, a freeform machining approach had to be applied. Therefore, the in-feed machining axis is synchronized to the angular and radial position of the freeform surface on the diamond turning machine's workpiece spindle to generate the freeform geometry. The forward and reverse motions are achieved by an additional kinematic tool holder of a low inertia device [Fast Tool Servo (FTS)]. The ultra-precision machining of high-frequency freeform surfaces using a voice coil driven FTS system is described by Scheiding et al.¹⁴

The programming of the tool path geometry relies on a point cloud description of the mold geometry. Therefore, the geometry must be translated into a format where the

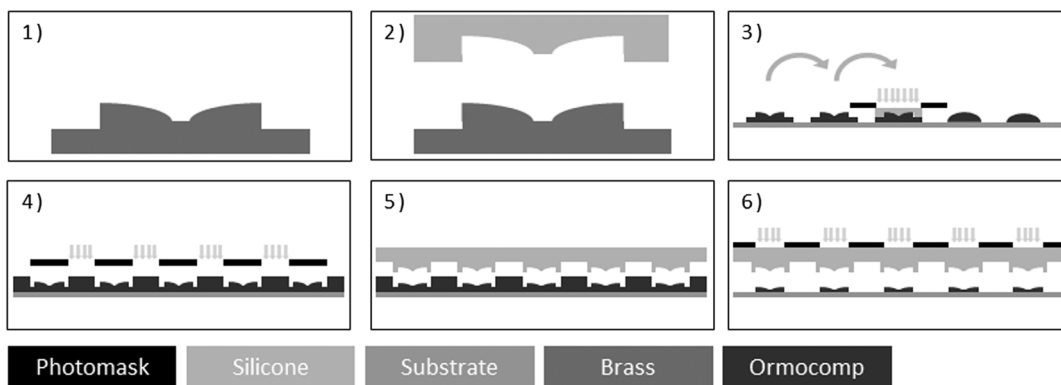


Fig. 3 Schematic drawing of the mastering process: (1) ultra-precision diamond machined brass master; (2) transparent silicone elastomer tool; (3) step and repeat process for the generation of an array of freeform micro-structures; (4) planarization of the array master; (5) array tool made of silicone elastomer by overcasting the master structure; and (6) UV-replication of the micro-structures on wafer level.

Table 1 Cutting data for the diamond turning of the master mold insert.

Cutting data	
Diamond tool radius r_e	350 μm
Depth of rough-cut a_p	>14 μm
Spindle speed	60 rpm
Feed rate	0.3 mm/min

stroke z is a function of the polar angle ϑ and the radial distance to the center of rotation r . The analytic description of the electrodes is developed in 1.8×10^6 points in a polar mesh with a radial spacing of 5 μm and an angular step of 0.18 deg. A radius compensation of the cutting tool is not necessary for this particular geometry since the radial slopes are equal to zero.

The total FTS-stroke required for the fabrication of the lens array is 14 μm . According to the frequency response specification of the manufacturer, the FTS is able to operate at >200 Hz at this amplitude.¹⁵ Assuming a constant spindle speed, the highest required frequency of the FTS is expected on the outer diameter. The possible spindle speed of >500 rpm is reduced to 60 rpm because the excitation does not follow a sinusoidal motion. To achieve a reasonably smooth surface, the feed per revolution is adjusted to be in

the micron range. The cutting data are summarized in Table 1.

The machining time for the whole geometry turned out to be 15 min. The micro-roughness of the diamond machined surface shows the typical turning structure overlaid with the grain structure of the brass substrate material. A roughness measurement using a white light interferometer (Zygo NewView 600, Middlefield, CT) with a 50 \times objective lens without filtering shows a micro-roughness of 5 nm (rms) in a field of 140 $\mu\text{m} \times 140 \mu\text{m}$.

4 Imprinting Results

The polynomial freeform derived from the FEA results was imprinted on wafer scale as shown in Fig. 3. The numbering of each single measurement is coincident with the numbering of the process steps in Fig. 3. After every single process step, the resulting freeform surface was measured with a white light interferometer (Zygo NewView 600) with 2.5 \times magnification. From this surface measurement, specific sections with different radii r were extracted [Fig. 4(a)], then plotted as diagram [Fig. 4(b)], and evaluated with respect to the deviation from the theoretical curvature. The curvature was designed with a 14- μm deflection starting at a height of 50 μm , and therefore ending at 36 μm preform height [Fig. 4(b)]. The initial value of 50 μm was solely a result of the semifinished preform and does not affect the intended deflection behavior or actuator design. The theoretical data points of the intended curvature of the preform are shown in Fig. 4(a).

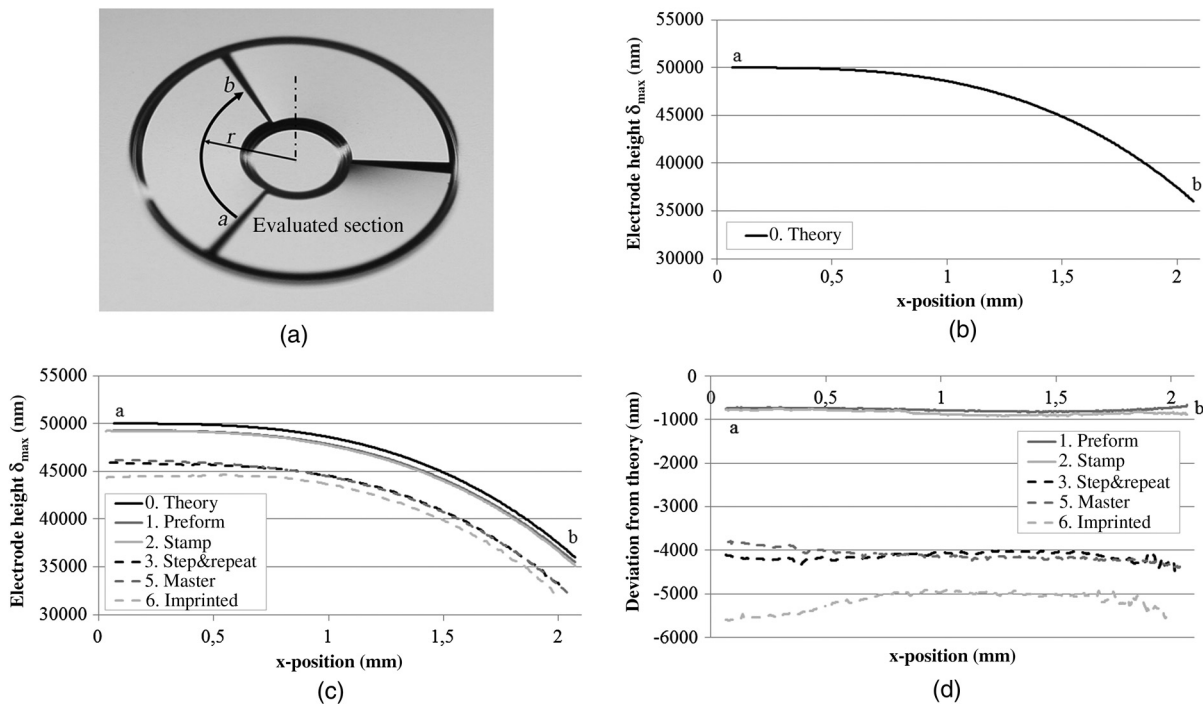


Fig. 4 (a) Example of an evaluated section with radius r . Letter “a” marks the starting point, letter “b” the end point of the curvature at which the deflection reaches the maximum of 14 μm . (b) Intended curvature derived from the FEA with a polynomial grade $n = 3$. The 14 μm falloff for electrode height starts at an elevation of 50 μm and ends at 36 μm . Both letters mark the start and end point of the section, respectively, as indicated in the picture top left. (c) Measurements of the curvature which was finally imprinted on an 8 in. glass substrate with the created array master (step 6 in Fig. 3) compared to the design, to the preform, to the replicated freeform (step and repeat), and the manufactured array master. The intermediate measurements are included and the numbering of each measurement is coincident with the process steps in Fig. 3. (d) Evaluation of the deviation between the designed and the final imprinted freeform, the intermediate measurements are included and the numbering of each measurement is coincident with the process steps in Fig. 3.

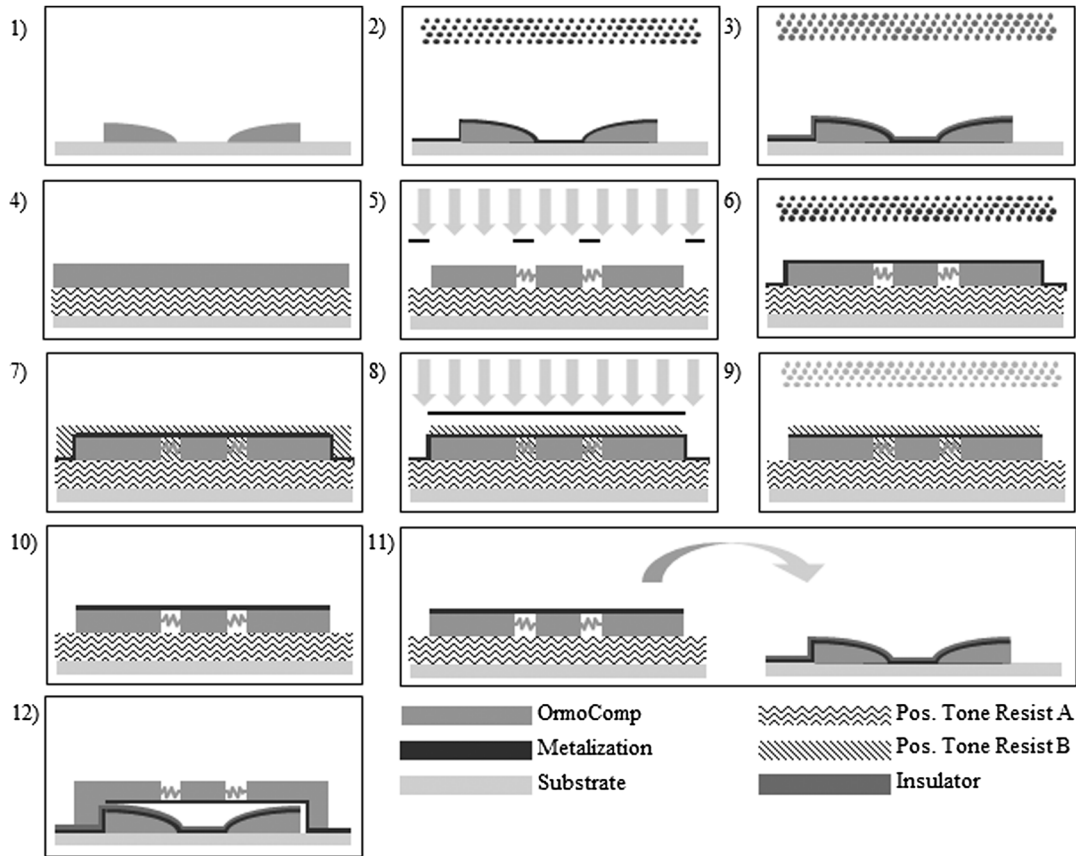


Fig. 5 Fabrication process steps of the polymer-based actuator with a freeform surface for an out-of-plane deflection.

Initially, the ultra-precision machined master was measured and evaluated as described. The offset of -700 nm from the intended electrode starting height of $50 \mu\text{m}$ is not critical as long as the quality of the curvature is maintained. Since the deflection and the shape of the surface are only defined by the curvature, the offset from the initial height will be neglected in the following evaluations. The surface deviation between the first measurement and the design values is 162 nm peak-to-valley (PV) and 30.7 nm root-mean-square (rms). In the final step, the array master was used to imprint the freeform in OrmoComp® on an 8 in. glass substrate as shown in step 6 of Fig. 3 [curvature measurements in Fig. 4(c)], resulting in a PV of 706.9 nm and an rms of 176.4 nm [Fig. 4(d)], respectively, for the final freeform. The quantity of deviation in step 6 is expected to be similar to step 3, due to the relatively soft silicone molds, which is confirmed by the measurements (increasing PV at about 101 nm and rms at about 76 nm, respectively). The whole fabrication process was successfully concluded with the wafer-level imprinted freeform of the intended curvature with $<1 \mu\text{m}$ PV and only 176 nm rms, respectively. It is noticeable that the steps in which a silicone mold is used to imprint OrmoComp® (Fig. 3, step 3 and step 6), showed the largest increase in deviation from the previous form. This can be explained by the relatively soft silicone being more sensitive to the imprinting parameters, which will be fine-tuned and improved with subsequent imprints.

5 Fabrication Process

The successful wafer-level imprinted freeform surfaces are compatible with the developed fabrication process which we

established in Ref. 16. The fabrication process for the whole actuator with integrated micro-mirror is shown in Fig. 5. Starting point is the imprinted freeform surface on a glass wafer (coincident with the result from Fig. 3, step 6). Then two basic lift off processes are used to structure a thin-film metallization (150 nm Ti) and an insulation layer ($2 \mu\text{m}$ SiO_2). A second wafer is spin-coated with photoresist A on which OrmoComp® is imprinted (step 4), UV-cured (step 5). A second metallization layer (150 nm Ti) is then sputtered on top (step 6) and structured by an etching process with a photoresist B as etching mask

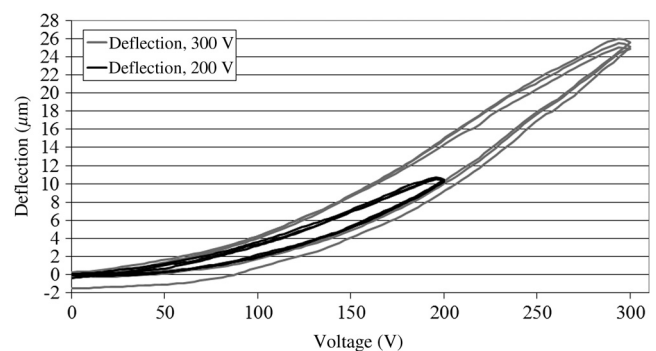


Fig. 6 Experimental results of the deflection versus voltage behavior. Due to fabrication-induced intrinsic stresses the beams are bent upward, resulting in a higher initial gap and therefore increased voltage. Instead of 60 V now 200 V are necessary for the intended deflection of $10 \mu\text{m}$. Although with only plus 100 V an overall deflection of $26 \mu\text{m}$ can be achieved.

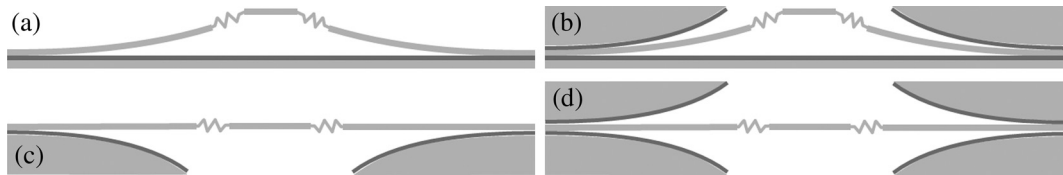


Fig. 7 Possible actuator designs based on a prebend zipper actuator and a minimal stress cantilever beam with a curved electrode. Type a: Zipper actuator as presented in Ref. 12, the fixed electrode is a flat surface, the cantilever beam is prebend to recreate the zipper principle. Type b: Prebend cantilever beam combined with an imprinted freeform, similar to the presented one. The additional polynomial curvature electrode is also able to increase the deflection of the whole zipper actuator, due to a possible actuation in two directions. Type c: Zipper actuator with a fixed polynomial curvature electrode with a low stress cantilever beam on top. This idea is presented in this paper. Type d: Extension to type (c) with a second pair of fixed polynomial curvature electrodes on top of the cantilever beam to double the deflection range of the actuator.

(steps 7–9). This photoresist B is then removed and due to the photoresist A on the second wafer the according Ormocomp® structure can be flipped and connected to the freeform structure of the first wafer (step 11), thus creating free standing cantilever beams for an electrostatic out-of-plane actuator.

Figure 5 shows this unconventional approach to fabricate electrostatic actuators that solely utilizes conventional UV-lithography and photomasks. The process is only realizable with a UV-curable polymer as base material. It is notable that all layers were structured without deposition through mechanical shadowmasks. Instead a lift-off or an etching process, based on conventional UV-lithography, was used. This makes it possible to use the positioning as well as feature size accuracy and resolution of lithographic photomasks. Additionally, and quite important for complex actuator designs, it is possible to mask isolated areas without the necessity of supporting bars. The width of conducting lines is limited only by photolithography and etching/lift-off process parameters.

6 Deflection Results

The measurement of the deflection-voltage dependency was run with a Keyence LK-G10 laser displacement sensor in the center area. A LabView-based software was used to control the voltage regime and measurements, ramping up the voltage in steps of 2, respectively 3 V with 200-ms interval between each in which the deflection was measured. After the peak of 200, respectively 300 V, the voltage was ramped down with the same parameters. This regime was repeated two additional times to ensure the reproducibility of the results, which are shown in Fig. 6 as deflection versus voltage.

With 200 V for actuation, the intended deflection of 10 μm was reached. The increased required voltage can be traced back to fabrication-induced intrinsic stresses, resulting in upward bent beams. This involves a greater possible deflection, so with 300 V an actual deflection of 26 μm is reached. With less than 1 μm deviation, the repeatability of the actuator performance is good and shows only a small hysteresis. Unfortunately, the increased initial gap does not allow a final conclusion if the analog behavior extends over the whole possible deflection range.

7 Conclusion and Outlook

In this paper, it is shown that the quality of the fabrication, replication, and wafer-level imprinting of a polynomial curvature is well suitable for the intended electrostatic actuator. Based on requirements derived from an exemplified

micro-mirror device, an actuator design was presented and polynomial curvature and cantilever geometries were derived. In this work, the successful array master molding and the imprinting of the required freeform surface on an 8 in. wafer with a PV of 706.9 nm and an rms surface roughness of 176.4 nm are described. The intended deflection of 10 μm was reached at a higher actuation voltage of 200 V due to the fabrication-induced intrinsic stresses and the resulting upward bending of the beams, allowing a higher maximum deflection, leading to a deflection of 26 μm at 300 V.

Reducing the intrinsic stresses to a minimum or even eliminating them completely is a difficult task or maybe not possible with a reasonable effort. Therefore, the intrinsic stresses and the resulting upward bending of the beams should be reflected in the future actuator design and combined with the ability to imprint polynomial curvature surfaces and freeforms, thus leading to a variation of possible actuator setups (Fig. 7).

The unusual and challenging approach to electrostatic actuators based on a nonconducting polymer offers very different advantages especially in comparison to silicon-based electrostatic actuators. The required actuation voltage is noticeably smaller due to the soft polymer and the polymer itself allows a whole new range of fabrication processes. Therefore, even complex freeform surfaces are possible and can be fabricated fast and cheap on a whole wafer in one process step only. With the layer-wise surface micromachining, each layer can be individually altered in the according process step. Due to the possibilities of imprinting freeform surfaces in polymer, the applications are not limited to micro-mirrors.

Acknowledgments

The work presented in this paper was funded by the Federal Ministry of Education and Research (BMBF) within the project “Active micro-optical subsystems for wafer-level processing-ActiveLens” (FKZ 16SV5018) and supervised by VDI/VDE-IT. Special thanks go to The Deutsche Forschungsgemeinschaft (DFG) for the support and networking opportunities within the priority program “Active Micro-optics” (SPP 1337).

References

1. W. S. N. Trimmer, “Microrobots and micromechanical systems,” *Sens. Actuators* **19**(3), 267–287 (1989).
2. H. Schenk, “Ein neuartiger Mikroaktor zur ein- und zweidimensionalen Ablenkung von Licht,” Dissertation, Gerhard-Mercator-Universität-Gesamthochschule, Duisburg, Germany (2000).
3. R. Legtenberg et al., “Electrostatic curved electrode actuators,” *J. Microelectromech. Syst.* **6**(3), 257–265 (1997).

4. H. Hanf et al., "Realization of electrostatically driven actuators using curved electrodes fabricated by using silicon bulk micromachining techniques," in *Proc. in 8th Int. Conf. on New Actuators*, pp. 329–332, Messe Bremen GmbH, Bremen, Germany (2002).
5. M. Hoffmann, D. Nüsse, and E. Voges, "Electrostatic parallel-plate actuators with large deflections for use in optical moving-fibre switches," *J. Micromech. Microeng.* **11**(4), 323–328 (2001).
6. J. Li, "Conventional zipping actuators," Chapter 2.21 in *Electrostatic Zipping Actuators and their Application to MEMS*, Ph.D. Thesis, pp. 34–35, Massachusetts Institute of Technology, Massachusetts (2004).
7. G. Perregaux et al., "Arrays of addressable high-speed optical micro-shutters," in *Proc. IEEE 14th Ann. Int. Conf. Microelectromechanical Systems*, pp. 232–235, IEEE Press, New York (2001).
8. R. Legtenberg, "Electrostatic curved electrode actuators," Chapter 5 in *Electrostatic Actuators Fabricated by Surface Micromachining Techniques*, Ph.D. Thesis, pp. 109–129, University of Twente, Twente (1996).
9. F. Sherman et al., "In-plane microactuator for fluid control," in *Proc. the Eleventh Annual International Workshop on Micro Electro Mechanical Systems*, pp. 454–459, IEEE Press, New York (1998).
10. C. Divoux et al., "A novel electrostatic actuator for micro deformable mirrors: fabrication and test," in *The 12th Int. Conf. on Solid State Sensors, Actuators and Microsystems*, pp. 488–491, IEEE Press, New York (2003).
11. C. Shizas and D. Karalekas, "Mechanical characteristics of an Ormocomp® biocompatible hybrid photopolymer," *J. Mech. Behav. Biomed. Mater.* **4**(1), 99–106 (2011).
12. R. Legtenberg, A. W. Groeneveld, and M. Elwenspoek, "Comb-drive actuators for large displacements," *J. Micromech. Microeng.* **6**(3), 320–329 (1996).
13. W. Ehrfeld and J. Bähr, *Handbuch Mikrotechnik: 47 Tabellen*, Hanser, München, Wien (2002).
14. S. Scheiding et al., "Freeform manufacturing of a microoptical lens array on a steep curved substrate by use of a voice coil fast tool servo," *Opt. Express* **19**(24), 23938–23951 (2011).
15. Moore Nanotechnology Systems, LLC, "NFTS-6000 Specification Overview," Product Brochure (2007).
16. N. Lange et al., "Innovative approach to high stroke electrostatic actuators," *SPIE Photonics West*, 2.-8.2.2013, San Francisco, California.



Nicolas Lange graduated in precision engineering from University for Applied Sciences in Jena in 2009. His work in the field of electrostatic zipper actuators based on polymers at the Fraunhofer Institute for Applied Optics and Precision Engineering (IOF) was the fundament for his position as a PhD student at the Friedrich-Schiller University in Jena. The topic of his thesis is electrostatic actuator simulation and fabrication based on UV-curable polymers on wafer level with integrated micro-optics. His main professional area is FEA and fabrication of actuators and polymer-based lithography.



Sebastian Scheiding received his diploma in mechanical engineering, with a focus on precision engineering and micro-technology, from the Technical University Berlin in 2007. As research associate at the Friedrich-Schiller-University in Jena and the Fraunhofer IOF his field of research included precision engineering with the focus on ultra-precision machining until 2013. The scope of his PhD thesis is the simplification of the system alignment of reflecting IR-telescopes based on metal optics. Since 2013, he is a chief technical officer (CTO) of Astro- und Feinwerktechnik Adlershof GmbH.



design especially in the field of wafer-level fabrication.

Frank Wippermann graduated from University for Applied Sciences in Jena in 1999. He worked in the field of fiber optical system design for sensing and telecommunication applications. In 2004, he joined the Fraunhofer Institute for Applied Optics and Precision Engineering (IOF) and finished his thesis on "Chirped micro-lens array configurations" in 2007. He is currently heading the Group of Micro-optical Imaging Systems. His main professional area is imaging optics



equipment development and manufacturing technologies for micro- and nanostructured opto-fluidic systems including printing and functionalization of smart materials.

Erik Beckert graduated from the Technical University Ilmenau in 1997. He received his PhD for his thesis, "Planar ceramic substrates and new assembly technologies for the packaging of hybrid optical systems," in 2005. Since 2005, he is a head of the micro-assembly and system integration group at Fraunhofer IOF. His research interest includes assembly and integration of optical and opto-mechatronic systems, advanced packaging technologies, assembly



Precision Engineering at the Fraunhofer IOF since 2005. Her experiences include precision fixation technologies like soldering and adhesive bonding, material sciences, and packaging of opto-mechanical systems.

Ramona Eberhardt received her diploma in chemistry in 1982 and PhD in 1987 from the Friedrich-Schiller University of Jena for her work about the thermo-optical properties of new developed phosphate glasses. After her PhD, she worked on the field of new glass solders for precise joining of optical and mechanical components. From 1992 to 2004, she was a group manager of the micro-assembly group at the Fraunhofer IOF, Jena. She has headed the Department



Fraunhofer Institute for Applied Optics and Precision Engineering IOF in Jena. Andreas Tünnermann is author of >400 papers in renowned international journals. He is a sought-after expert in optics and photonics industry. His research activities on applied quantum electronics have been awarded, e.g., with the Gottfried-Wilhelm-Leibniz-Award (2005). In 2013, he became a fellow of SPIE.

Andreas Tünnermann received the diploma and PhD degrees in physics from the University of Hannover in 1988 and 1992, respectively. In 1997, he received the habilitation. He was head of the Department of Development at the Laser Zentrum Hannover from 1992 to 1997. In the beginning of 1998, he joined the Friedrich-Schiller-University in Jena, Germany, as a professor and director of the Institute of Applied Physics. In 2003, he was appointed as the director of the